PAPER

Effect of CoFe dusting layer and annealing on the magnetic properties of sputtered Ta/W/CoFeB/CoFe/MgO layer structures

View the article online for updates and enhancements.

Effect of CoFe dusting layer and annealing on the magnetic properties of sputtered Ta/W/CoFeB/CoFe/MgO layer structures

J L Drobitch[1,2] **, Y-C Hsiao**[3]**, H Wu**[4]**, K L Wang**[4]**, C S Lynch**[5]**, K Bussmann**[6]**, S Bandyopadhyay**[1] **and D B Gopman**[2,7]

[1] Electrical and Computer Engineering Department, Virginia Commonwealth University, Richmond, VA, United States of America
[2] Materials Science and Engineering Division, National Institute of Standards and Technology, Gaithersburg, MD, United States of America
[3] Mechanical and Aerospace Engineering, University of California, Los Angeles, Los Angeles, CA, United States of America
[4] Electrical and Computer Engineering Department, University of California, Los Angeles, Los Angeles, CA, United States of America
[5] College of Engineering, University of California at Riverside, Riverside, CA, United States of America
[6] US Naval Research Laboratory, Washington, DC, United States of America

E-mail: daniel.gopman@nist.gov

CrossMark

Abstract

We explored the effect of a CoFe wedge inserted as a dusting layer (0.2 nm–0.4 nm thick) at the CoFeB/MgO interface of a sputtered Ta(2 nm)/W(3 nm)/CoFeB(0.9 nm)/MgO(3 nm)/Ta(2 nm) film—a typical structure for spin-orbit torque devices. Films were annealed at temperatures varying between 300 °C and 400 °C in an argon environment. Ferromagnetic resonance studies and vibrating sample magnetometry measurements were carried out to estimate the effective anisotropy field, the Gilbert damping, the saturation magnetization and the dead layer thickness as a function of the CoFe thickness and across several annealing temperatures. While the as-deposited films present only easy-plane anisotropy, a transition along the wedge from in-plane to out-of-plane was observed across several annealing temperatures, with evidence of a spin-reorientation transition separating the two regions.

Keywords: spintronics, perpendicular magnetic anisotropy, CoFeB, annealing, ferromagnetic resonance, gilbert damping

S Supplementary material for this article is available online

(Some figures may appear in colour only in the online journal)

1. Introduction

Ultrathin CoFeB films have been essential to many spintronic applications since the discovery of perpendicular magnetic anisotropy in CoFeB/MgO magnetic tunnel junctions [1]. Perpendicular magnetic anisotropy (PMA) is critical for achieving next-generation high density spintronic devices

with low power consumption due to the achievability of high thermal stability and low critical switching current [2, 3]. Manipulating magnetic properties of ultrathin CoFeB films through interface engineering is an area of intense research within the spintronics community.

Properties are highly dependent on the choice of layer structure, and many studies have focused on the effects and optimization of various top and bottom film structures [4–7]. Layered CoFeB/MgO structures with heavy metal

[7] Author to whom any correspondence should be addressed.

J. Phys. D: Appl. Phys. **53** (2020) 105001

J L Drobitch *et al*

underlayers, particularly tungsten, were shown to have strong PMA, low Gilbert damping, and high thermal stability [6–9]. Interfacial anisotropy is found to be greater with a W buffer compared to a Ta buffer [10]. Thin capping layers of Ta were also shown to increase interfacial anisotropy [11, 12]. Devices must maintain characteristics and performance over a range of annealing temperatures up to 400 °C, a standard compatibility requirement for CMOS processing.

Here we look at insertion of very thin CoFe layer at the CoFeB/MgO interface to determine its effect on the underlying magnetic properties and annealing stability—key factors for spintronic applications involving CoFeB. The CoFe insertion layer thickness varies continuously along the 60 mm long axis of a rectangular Si substrate, providing thinner regions with perpendicular magnetization and thicker regions whose magnetization lies within the sample plane. The success of this approach was demonstrated in samples annealed at temperatures exceeding 350 °C. In fact, the sample annealed at 400 °C exhibited regions in which our measurements estimated a modest perpendicular magnetic anisotropy energy. The role of CoFe thickness on the magnetic and annealing properties will be discussed.

2. Experimental

Samples were produced in which an ultrathin CoFe wedge layer was inserted between the CoFeB and MgO layers in a thin film heterostructure grown on a thermally oxidized Si substrate. Each layer of the deposited film was grown by direct current at constant power (100 W) (excepting the MgO layer, grown by radio frequency at 150 W) magnetron sputtering at room temperature in a chamber with base pressure less than 1.3×10^{-6} Pa (1.0×10^{-8} Torr) and a working Ar pressure of 0.4 Pa (3 mTorr). Each sputtering target (CoFe, Ta, CoFeB, MgO) was a $2''$ sputtering target. The structure of the sample was Ta (2 nm)/W (3 nm)/$Co_{20}Fe_{60}B_{20}$ (0.9 nm)/$Co_{50}Fe_{50}$ (0.2 nm–0.4 nm)/MgO (3 nm)/Ta (2 nm). Nominal film deposition rates were estimated from calibration samples, and thicknesses were confirmed from x-ray reflectivity measurements of the wedge sample (see supplementary information (stacks. iop.org/JPhysD/53/105001/mmedia)). The calibrated deposition rates (Å s^{-1}) are: CoFe (0.34); Ta (0.5); CoFeB (0.32) and MgO (0.06). Ta, CoFeB, and MgO layers were grown with the substrate surface normal confocal with the sputtering targets. However, the CoFe layer was deposited after having translated the center of the substrate manipulator to a displacement that is 45° away from the sputtering gun surface normal. Such an oblique orientation enabled us to obtain a continuously varying CoFe layer along the direction of the substrate oriented radially outward from the focus of the CoFe sputtering gun. Calibration of the nominal thicknesses of the thickness wedge described in this manuscript was carried out on a much thicker CoFe wedge calibration sample, whose x-ray reflectivity results are included in the supplementary information.

In order to promote depletion of the B-content in CoFeB and to promote crystallization of the CoFeB, CoFe, and MgO layers, samples were annealed post-deposition using a rapid
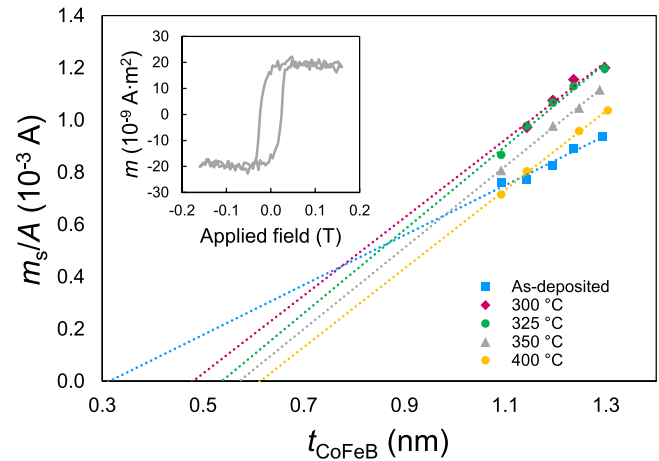

Figure 1. Saturation moment per unit area. Dead layer thickness and saturation magnetization were extracted from the x-intercept and slope, respectively. Inset: magnetic moment for sample with combined CoFeB/CoFe thickness of 1.20 nm annealed at 350 °C.

thermal annealer (RTA) [4, 13, 14]. Annealing was carried out in an argon environment for 30 min at 300 °C, 325 °C, 350 °C, and 400 °C, temperatures known to induce crystallization and promote perpendicular magnetic anisotropy [7, 15]. Individual samples were cleaved from the wedge at representative positions along the thickness gradient to evaluate the role of CoFe insertion layer thickness on magnetic properties and the effects of annealing.

Magnetic properties of both the as-deposited and annealed samples were measured with a vibrating sample magnetometer (VSM) and broadband ferromagnetic resonance (FMR). Estimation of the saturation magnetization and magnetic dead layer thickness were carried out using a Microsense VSM[8]. Magnetic moment was measured along the applied field direction with fields applied within the plane of the film. Measurements of the ferromagnetic resonance field and linewidth versus frequency were taken to estimate the perpendicular anisotropy field and Gilbert damping in the films. Samples were placed film-side down on a coplanar waveguide within an electromagnet with a field range up to 1.5 T and frequency excitation range 1–50 GHz [16]. All measurements were conducted with the applied magnetic field aligned in the plane of the thin film samples.
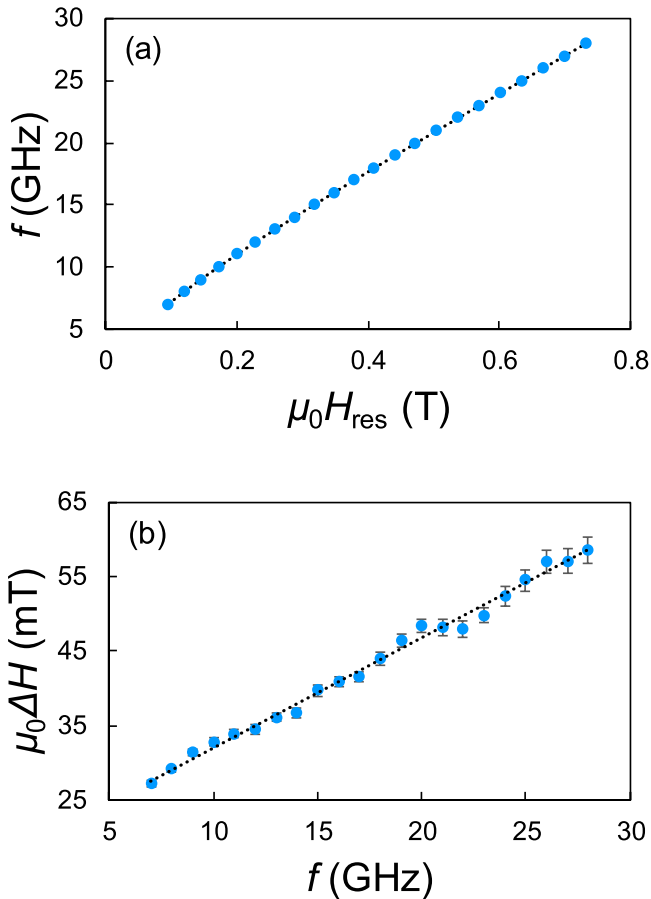
3. Results and discussion

Magnetometry was used to evaluate the saturation magnetization and dead layer thickness amongst the samples and under the various annealing conditions. Magnetic moment was measured along the applied field direction with fields applied within the film plane. The saturation moment was estimated for each sample from its magnetic hysteresis loop; an example is given

---

[8] Certain commercial equipments are identified in this paper to foster understanding of the experimental details. Such identification does not imply recommendation or endorsement by the coauthors, nor does it imply that the materials or equipment identified are necessarily the best available for the purpose.
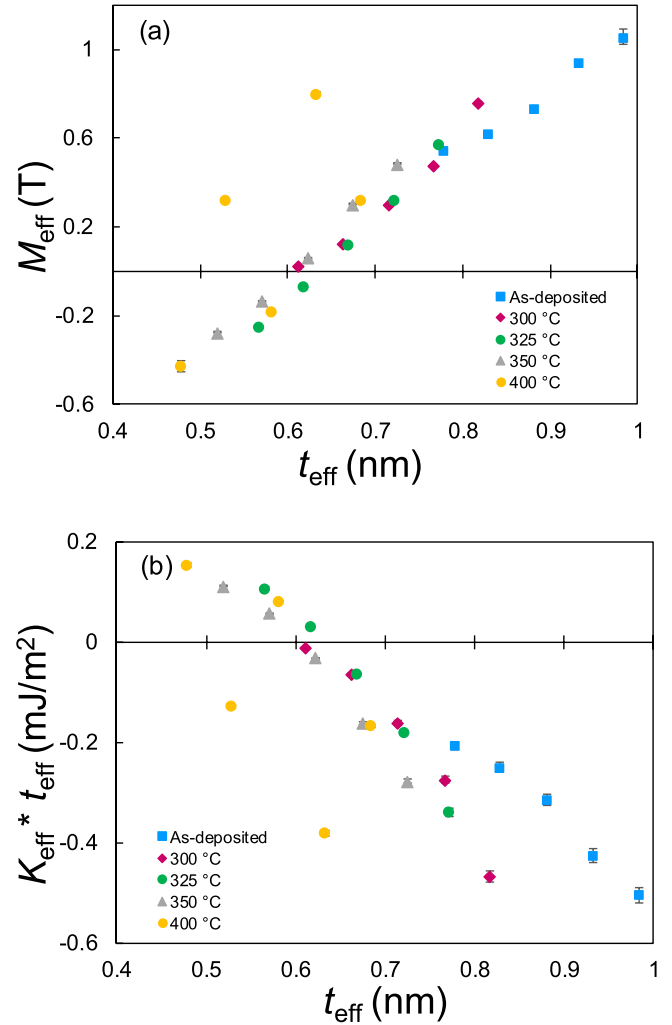
J. Phys. D: Appl. Phys. **53** (2020) 105001

J L Drobitch *et al*

Table 1. Dead layer thickness (t_{DL}) and saturation magnetization (M_S) for CoFeB/CoFe/MgO heterostructures for several annealing conditions.

	t_{DL} (nm)	M_S (kA m^{-1})
As-deposited	0.32 ± 0.03	970 ± 30
300 °C	0.48 ± 0.02	1500 ± 40
325 °C	0.54 ± 0.02	1600 ± 30
350 °C	0.57 ± 0.01	1570 ± 30
400 °C	0.62 ± 0.01	1510 ± 30

Figure 3. (a) Effective demagnetization field versus effective thickness (combined CoFeB/CoFe layer thickness minus dead layer thickness) for several annealing temperatures. (b) Effective magnetic anisotropy multiplied by effective thickness versus the effective thickness for several annealing temperatures.

Figure 2. (a) The ferromagnetic resonance field versus excitation frequency and (b) the linewidth versus excitation frequency of the sample with combined CoFeB and CoFe thickness t = 1.26 nm annealed at 350 °C.

in figure 1 (inset) for the 1.20 nm thick sample annealed at 350 °C, and magnetic hysteresis plots for all samples are available in the Supplementary data provided. The areal saturation magnetization was plotted against the combined thickness of the CoFeB and CoFe layers, as shown in figure 1.

For each of the sample series under various annealing conditions, a non-zero horizontal asymptote in the areal moment versus thickness curve indicates the presence of a magnetic dead layer, commonly seen in CoFeB/MgO thin films [5, 10]. From the data in figure 1, we evaluated the dead layer thickness (the *x*-intercept) and the saturation magnetization (the slope) for each annealing series. A clear trend shows that the dead layer thickness increases with annealing, while the saturation magnetization only increases up to 325 °C, after

which it appears to level off or slightly decrease. This trend has been seen in homogeneous CoFeB layers and is typically associated with the oxidation of the CoFe at the MgO interface and interdiffusion with the heavy metal underlayer (W in this case), and the densification of the CoFe layer during annealing, respectively [4, 14, 17].

Estimates for dead layer thickness, t_{DL}, and saturation magnetization, M_S, are summarized in table 1. Uncertainty in the estimated parameters reflect uncertainties in the measured areal saturation magnetization, uncertainty in the nominal film thickness, and the variance of the parameter estimates from linear fitting of the areal magnetization versus nominal thickness data. The dead layer thickness increased from 0.48 nm to 0.62 nm for annealing temperatures from 300 °C to 400 °C—observations that agree with results from other groups [7, 9, 14]. Our results indicate a saturation magnetization of approximately 1500 kA m^{-1} was achieved by annealing at 300 °C, which is larger than previous results without a CoFe insertion layer for this annealing temperature [7, 9, 14].
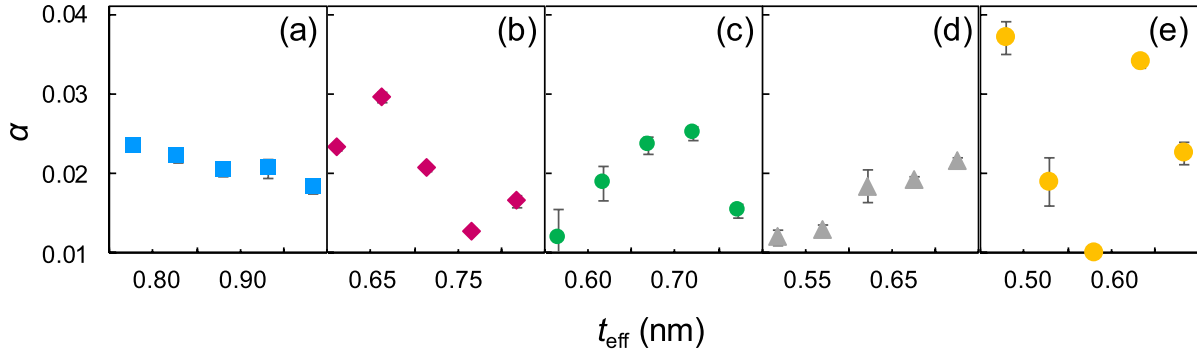
J. Phys. D: Appl. Phys. **53** (2020) 105001

J L Drobitch *et al*

Figure 4. Gilbert damping coefficient for annealing temperatures of (a) as-deposited, (b) 300 °C, (c) 325 °C, (d) 350 °C, and (e) 400 °C as a function of effective thickness of combined CoFeB/CoFe layer.

Next, ferromagnetic resonance measurements were taken to estimate the perpendicular anisotropy field and Gilbert damping in the films. For each sample, a series of absorption versus applied field scans were taken at several frequencies to sample the ferromagnetic resonance field versus frequency dispersion and the linewidth versus frequency dispersion. Additional data and details on parameter estimation are provided in the supplementary information. The ferromagnetic resonance condition is given by the Kittel equation for planar applied fields [18]:

$$f^2 = \gamma^2 \mu_0^2 H \left(H + M_S - \frac{2K_1}{M_S} - \frac{4K_2}{M_S} \right) \quad (1)$$

where γ is the gyromagnetic ratio, M_S is the saturation magnetization, and K_1 and K_2 are the first and second order uniaxial anisotropy constants. The linewidth of the resonance is linear in frequency:

$$\mu_0 \Delta H = \frac{2\alpha f}{\gamma} + \mu_0 \Delta H_0 \quad (2)$$

where $\mu_0 H_0$ is the inhomogeneous linewidth broadening and α is the Gilbert damping coefficient. Exemplary data is presented in figure 2 for the sample with combined CoFeB and CoFe thickness $t = 1.26$ nm annealed at 350 °C, with best-fit curves overlaid on top of the data markers. The Kittel equation is used to fit the data and extract the effective magnetization, M_{eff}:

$$\mu_0 M_{\text{eff}} = \mu_0 M_S - 2K_1/M_S - 4K_2/M_S. \quad (3)$$

The effective magnetization versus the effective thickness (defined as the combined CoFeB and CoFe thickness minus the dead layer thickness at each temperature) has been plotted in figure 3(a). Vertical error bars reflect the one-sigma uncertainty in the M_{eff} parameter estimated from the frequency versus resonance field dispersion, which implicitly carries the uncertainties of each estimated resonance field from Lorentzian fits to the absorption curve and ultimately, the precision of the applied external field. For the as-deposited sample, all discrete points along the CoFe thickness wedge revealed a positive effective magnetization, and correspondingly an easy-plane magnetization. As the annealing temperature is increased, the magnetic dead layer thickness similarly rises. However, the position of the thickness-dependent transition between an easy-plane and an out-of-plane magnetic easy axis takes

place around a common effective thickness of approximately 0.63 nm. This is a strong indication that the appearance of perpendicularly magnetized regions of the nominally higher combined CoFeB and CoFe thicknesses at elevated annealing temperatures is strongly influenced by the corresponding increases in magnetic dead layer thickness with annealing temperature. A net perpendicular magnetic anisotropy was observed in several regions of the samples annealed at 325 °C, 350 °C, and 400 °C with CoFe insertion layer effective thicknesses ($t_{\text{CoFeB}} - t_{\text{DL}}$) below 0.7 nm. While a thickness dependence consistent with an interfacial anisotropy is observed for temperatures up to 350 °C, the M_{eff} versus thickness for the sample annealed at 400 °C is clearly non-monotonic. This appears to be a reliability issue associated with annealing stability in the heterogeneous CoFe/CoFeB samples at 400 °C.

By plotting the M_{eff} data versus the effective thickness instead of the nominal thickness, we can see that the annealing series nearly collapse onto a master curve. Here we can estimate that the zero-crossing (the spin reorientation transition into the plane) occurs in the vicinity of an effective thickness of 0.6 nm. In particular, the critical effective thickness is 0.62 nm for an annealing temperature of 300 °C, 0.63 nm for an annealing temperature of 325 °C, 0.59 nm for an annealing temperature of 350 °C, and finally 0.60 nm for annealing at 400 °C. Interestingly, measurements of the effective magnetization in the two sample series annealed at 325 °C and 350 °C are qualitatively very similar, indicating a range of annealing temperature stability over which the magnetic anisotropy variation is minimal.

The effective magnetic anisotropy multiplied by effective thickness versus the effective thickness has been plotted in figure 3(b). Effective magnetic anisotropy is given by:

$$K_{\text{eff}} = -\frac{1}{2} M_{\text{eff}} M_S. \quad (4)$$

We estimate K_i by a linear fit to the $K_{\text{eff}} * t_{\text{eff}}$ versus t_{eff} data shown in figure 3(b), for which the y-intercept value equals K_i. K_i values are 0.98, 1.36, 1.35, and 1.15 mJ m^{-2} for the as-deposited, 300 °C, 325 °C, and 350 °C annealing temperatures, respectively.

The Gilbert damping (α) parameter versus effective thickness of the CoFeB/CoFe layer is shown in figure 4. Vertical error bars reflect the one-sigma uncertainty in the

J. Phys. D: Appl. Phys. **53** (2020) 105001

J L Drobitch *et al*

α parameter estimated from the linewidth versus frequency dispersion, which implicitly carries the uncertainties of each estimated resonance linewidth from Lorentzian fits to the absorption curve and ultimately, the precision of the applied external field. The overall average magnitude of the Gilbert damping is comparable with similar CoFeB films grown without a CoFe dusting layer, and there is a moderate reduction in the damping following annealing [9]. Thinner CoFe insertion layer samples show a net reduction in the Gilbert damping upon annealing up to 350 °C, when compared to the as-deposited case. On the other hand, samples with a thicker CoFe insertion layer exhibit a weaker temperature trend, or do not indicate a significant change in the Gilbert damping under annealing. This suggests that the annealing treatment has a weaker effect on the samples with a thicker CoFe insertion, and perhaps serves as an indication of the significance of the relatively higher boron content in the annealing and crystallization of thinner layers and thereby on the damping behavior.

The effective demagnetization data and the Gilbert damping constant estimated from the 400 °C annealed thickness series has a clearly non-monotonic trend, in contrast to the other samples in this growth series. Possible reasons for this range from overoxidation through the thin (2 nm thick) Ta cap to thermodynamic instability of this particular heterostructure, leading to the deleterious effects of interdiffusion of the W/CoFeB/CoFe complex. This may suggest that for the particular sample series, the annealing stability is limited to below 400 °C.

4. Conclusion

This study has demonstrated the feasibility of using a dusting layer of CoFe at the interface between CoFeB and MgO to achieve moderate perpendicular magnetic anisotropy, low damping, and relatively high saturation magnetization. For several annealed samples, we observed a net perpendicular magnetic anisotropy with a saturation magnetization exceeding 1500 kA m^{-1} and a Gilbert damping coefficient below 0.015.

Engineering desirable spintronic properties in the CoFeB/MgO system follows from depositing a Co–Fe–B alloy layer that is sufficiently amorphous and dense to form a smooth underlayer for the MgO growth, followed by crystallization during annealing under the influence of the MgO layer. Previous studies have looked at the effect of boron composition in Co–Fe–B layers on several paraments including microstructure, magnetic anisotropy, and annealing stability [19–21]. By inserting a CoFe layer between the CoFeB and MgO, we demonstrate an approach for introducing a thickness gradient in B content, which can modify the final properties of the annealed bilayer by changing the microstructure of the as-deposited film. Future studies may indicate that not only the proportion of CoFe to CoFeB, but the location of the inserted CoFe layer within the CoFeB film could have meaningful effects on the properties of annealed heterostructures.

ORCID iDs

J L Drobitch ⓘ https://orcid.org/0000-0002-4439-7551
S Bandyopadhyay ⓘ https://orcid.org/0000-0001-6074-1212
D B Gopman ⓘ https://orcid.org/0000-0003-4172-8113

References

[1] Ikeda S, Miura K, Yamamoto H, Mizunuma K, Gan H D, Endo M, Kanai S, Hayakawa J, Matsukura F and Ohno H 2010 A perpendicular-anisotropy CoFeB–MgO magnetic tunnel junction *Nat. Mater.* **9** 721–4

[2] Kishi T *et al* 2008 Lower-current and fast switching of A perpendicular TMR for high speed and high density spin-transfer-torque MRAM *Technical Digest—Int. Electron Devices Meeting* (https://doi.org/10.1109/IEDM.2008.4796680)

[3] Nishimura N, Hirai T, Koganei A, Ikeda T, Okano K, Sekiguchi Y and Osada Y 2002 Magnetic tunnel junction device with perpendicular magnetization films for high-density magnetic random access memory *J. Appl. Phys.* **91** 5246–9

[4] Wang Y-H, Chen W-C, Yang S-Y, Shen K-H, Park C, Kao M-J and Tsai M-J 2006 Interfacial and annealing effects on magnetic properties of CoFeB thin films *J. Appl. Phys.* **99** 08M307

[5] Jang S Y, Lim S H and Lee S R 2010 Magnetic dead layer in amorphous CoFeB layers with various top and bottom structures *J. Appl. Phys.* **107** 09C707

[6] Torrejon J, Kim J, Sinha J, Mitani S, Hayashi M, Yamanouchi M and Ohno H 2014 Interface control of the magnetic chirality in CoFeB/MgO heterostructures with heavy-metal underlayers *Nat. Commun.* **5** 4655

[7] An G-G, Lee J-B, Yang S-M, Kim J-H, Chung W-S and Hong J-P 2015 Highly stable perpendicular magnetic anisotropies of CoFeB/MgO frames employing W buffer and capping layers *Acta Mater.* **87** 259–65

[8] Lee K-M, Choi J W, Sok J and Min B-C 2017 Temperature dependence of the interfacial magnetic anisotropy in W/CoFeB/MgO *AIP Adv.* **7** 065107

[9] Lattery D M, Zhang D, Zhu J, Hang X, Wang J-P and Wang X 2018 Low Gilbert damping constant in perpendicularly magnetized W/CoFeB/MgO films with high thermal stability *Sci. Rep.* **8** 13395

[10] Watanabe K, Fukami S, Sato H, Ikeda S, Matsukura F and Ohno H 2017 Annealing temperature dependence of magnetic properties of CoFeB/MgO stacks on different buffer layers *Japan. J. Appl. Phys.* **56** 0802B2

[11] Cheng C W, Feng W, Chern G, Lee C M and Wu T H 2011 Effect of cap layer thickness on the perpendicular magnetic anisotropy in top MgO/CoFeB/Ta structures *J. Appl. Phys.* **110** 033916

[12] Kim D, Jung K Y, Joo S, Jang Y, Hong J, Lee B C, You C Y, Cho J H, Kim M Y and Rhie K 2015 Perpendicular magnetization of CoFeB on top of an amorphous buffer layer *J. Magn. Magn. Mater.* **374** 350–3

[13] Ikeda S, Hayakawa J, Ashizawa Y, Lee Y M, Miura K, Hasegawa H, Tsunoda M, Matsukura F and Ohno H 2008 Tunnel magnetoresistance of 604% at 300 K by suppression of Ta diffusion in CoFeBMgOCoFeB pseudo-spin-valves annealed at high temperature *Appl. Phys. Lett.* **93** 082508

J. Phys. D: Appl. Phys. **53** (2020) 105001

J L Drobitch *et al*

[14] Jang S Y, You C Y, Lim S H and Lee S R 2011 Annealing effects on the magnetic dead layer and saturation magnetization in unit structures relevant to a synthetic ferrimagnetic free structure *J. Appl. Phys.* **109** 013901

[15] Skowroński W, Nozaki T, Lam D D, Shiota Y, Yakushiji K, Kubota H, Fukushima A, Yuasa S and Suzuki Y 2015 Underlayer material influence on electric-field controlled perpendicular magnetic anisotropy in CoFeB/MgO magnetic tunnel junctions *Phys. Rev.* B **91** 184410

[16] Gopman D B, Sampath V, Ahmad H, Bandyopadhyay S and Atulasimha J 2017 Static and dynamic magnetic properties of sputtered Fe–Ga thin films *IEEE Trans. Magn.* **53** 6101304

[17] Oguz K, Jivrajka P, Venkatesan M, Feng G and Coey J M D 2008 Magnetic dead layers in sputtered $Co_{40}Fe_{40}B_{20}$ films *J. Appl. Phys.* **103** 07B526

[18] Kittel C 1948 On the theory of ferromagnetic resonance absorption *Phys. Rev.* **73** 155–61

[19] Kodzuka M, Ohkubo T, Hono K, Ikeda S, Gan H D and Ohno H 2012 Effects of boron composition on tunneling magnetoresistance ratio and microstructure of CoFeB/MgO/CoFeB pseudo-spin-valve magnetic tunnel junctions *J. Appl. Phys.* **111** 043913

[20] Ikeda S, Koizumi R, Sato H, Yamanouchi M, Miura K, Mizunuma K, Gan H, Matsukura F and Ohno H 2012 Boron composition dependence of magnetic anisotropy and tunnel magnetoresistance in MgO/CoFe(B) based stack structures *IEEE Trans. Magn.* **48** 3829–32

[21] Honjo H *et al* 2016 Improvement of thermal tolerance of CoFeB–MgO perpendicular-anisotropy magnetic tunnel junctions by controlling boron composition *IEEE Trans. Magn.* **52** 3401104